J|A|C|S
ARTICLES

Unsaturated Platinum−Rhenium Cluster Complexes. Synthesis, Structures and Reactivity

Richard D. Adams,*,[†] Burjor Captain,[†] Mark D. Smith,[†] Chad Beddie,[‡] and
Michael B. Hall*,[‡]

*Contribution from the Department of Chemistry and Biochemistry, University of South Carolina,
Columbia, South Carolina 29208, and Department of Chemistry, Texas A&M University,
College Station, Texas 77843-3255*

Received February 2, 2007; E-mail: adams@mail.chem.sc.edu

Abstract: Two new compounds $PtRe_3(CO)_{12}(PBu^t_3)(\mu\text{-}H)_3$, **9**, and $PtRe_2(CO)_9(PBu^t_3)(\mu\text{-}H)_2$, **10**, were obtained from the reaction of $Pt(PBu^t_3)_2$ with $Re_3(CO)_{12}(\mu\text{-}H_3)$, **8**, at room temperature. Compound **9** contains a butterfly cluster of four metals formed by the insertion of the platinum atom from a $Pt(PBu^t_3)$ group into one of the hydride-bridged metal−metal bonds of **8**. The three hydrido ligands are bridging ligands across each of three new Pt−Re bonds. Compound **10** contains a triangular $PtRe_2$ cluster with two hydrido ligands; one bridges a Pt−Re bond, and the other bridges the Re−Re bond. The new compound $Pt_2Re_2(CO)_7(PBu^t_3)_2(\mu\text{-}H)_2$, **11**, was obtained from the reaction of **8** with $Pt(PBu^t_3)_2$ in hexane at reflux. Compound **11** was also obtained from **10** by reaction with an additional quantity of $Pt(PBu^t_3)_2$. Compound **11** contains a tetrahedral cluster of four metal atoms with two dynamically active hydrido ligands. A CO ligand on one of the two platinum atoms also exchanges between the two platinum atoms rapidly on the NMR time scale. Compound **11** is electronically unsaturated and was found to add hydrogen at room temperature to form the tetrahydrido cluster complex, $Pt_2Re_2(CO)_7(PBu^t_3)_2(\mu\text{-}H)_4$, **12**. Compound **12** has a structure similar to **11** but contains one triply bridging hydrido ligand, two edge bridging hydrido ligands, and one terminal hydrido ligand on one of the two platinum atoms. A kinetic isotope effect D/H of 1.5(1) was determined for the addition of H_2 to **11**. Hydrogen can be eliminated from **12** by heating to 97 °C or by the application of UV−vis irradiation at room temperature. Compound **12** adds CO at room temperature to yield the complex $Pt_2Re_2(CO)_8(PBu^t_3)_2(\mu\text{-}H)_4$, **13**, which contains a planar cluster of four metal atoms with a Pt−Pt bond and four edge bridging hydrido ligands. Compounds **11** and **12** react with $Pt(PBu^t_3)_2$ to yield the known five metal cluster complexes $Pt_3Re_2(CO)_6(PBu^t_3)_3(\mu\text{-}H)_2$, **14**, and $Pt_3Re_2(CO)_6(PBu^t_3)_3(\mu\text{-}H)_4$, **15**, respectively. Density functional calculations confirm the hydride positions in the lowest energy structural isomers of **11** and **12** and suggest a mechanism for H_2 addition to **11** that occurs on the Pt atom with the lower coordination number.

Introduction

In recent studies we have shown that metal containing groupings $M(PBu^t_3)$, M = Pd and Pt, obtained from the precursors $M(PBu^t_3)_2$, M = Pd and Pt, are readily added to the metal−metal bonds of polynuclear metal carbonyl cluster complexes to form electron-deficient adducts containing bridging $M(PBu^t_3)$ groups. For example, the reaction of $M(PBu^t_3)_2$, M = Pd and Pt, with $Ru_3(CO)_{12}$ and $Os_3(CO)_{12}$ yield tri-$M(PBu^t_3)$ adducts: $Ru_3(CO)_{12}[Pd(PBu^t_3)]_3$, **1**,[1] and $Os_3(CO)_{12}[Pt(PBu^t_3)]_3$, **2**.[2]

$Pd(PBu^t_3)_2$ and $Pt(PBu^t_3)_2$ also react with $Ru_5(CO)_{15}(\mu_5\text{-}C)$ to afford the adducts $Ru_5(CO)_{15}(C)[M(PBu^t_3)]$, **3**, M = Pd, and **4**, M = Pt. Compounds **3** and **4** both exist in solution as a mixture of open and closed isomers (e.g., **4a** and **4b**) that interconvert rapidly on the NMR time scale at room temperature.[3] $Pt(PBu^t_3)_2$ reacts with $Ir_4(CO)_{12}$ to yield the di-$Pt(PBu^t_3)$ adduct $Pt_2Ir_4(CO)_{12}(PBu^t_3)_2$, **5**.[4]

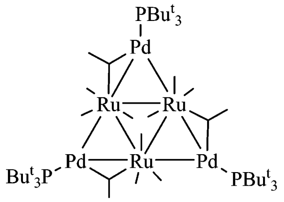

1

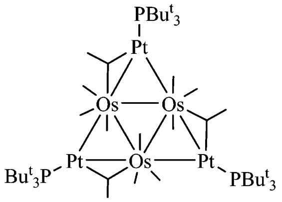

2

Platinum-rhenium bimetallic catalysts have attracted great interest because of their superior properties for the important process of petroleum reforming.[5] Recent studies have shown

---

[†] University of South Carolina.

[‡] Texas A&M University.

(1) (a) Adams, R. D.; Captain, B.; Fu, W.; Hall, M. B.; Manson, J.; Smith, M. D.; Webster, C. E. *J. Am. Chem.* Soc. **2004**, *126*, 5253−5267. (b) Adams, R. D.; Captain, B.; Fu, W.; Smith, M. D. *J. Am. Chem.* Soc. **2002**, *124*, 5628−5629.

(2) Adams, R. D.; Captain, B.; Zhu, L. *Inorg. Chem.* **2006**, *45*, 430−436.

(3) (a) Adams, R. D.; Captain, B.; Fu, W.; Pellechia, P. J.; Smith, M. D. *Angew. Chem., Int. Ed.* **2002**, *41*, 1951−1953. (b) Adams, R. D.; Captain, B.; Fu, W.; Pellechia, P. J.; Smith, M. D. *Inorg. Chem.* **2003**, *42*, 2094−2101.

(4) Adams, R. D.; Captain, B.; Hall, M. B.; Smith, J. L., Jr.; Webster, C. E. *J. Am. Chem. Soc.* **2005**, *127*, 1007−1014.

10.1021/ja070773o CCC: $37.00

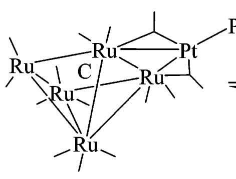

4a

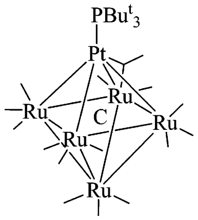

4b

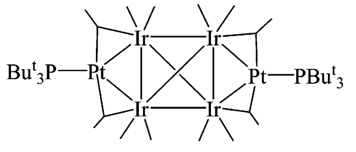

5

that unsaturated polynuclear metal complexes containing bulky phosphine ligands can absorb relatively large amounts of hydrogen under mild conditions.[6] We have recently prepared the new highly unsaturated platinum−rhenium complex $Pt_3Re_2(CO)_6(PBu^t_3)_2$, **6**, that readily adds 3 equiv of hydrogen at room temperature to yield the hexahydrido complex $Pt_3Re_2(CO)_6(PBu^t_3)_3(\mu\text{-}H)_6$, **7**, eq 1.[7]

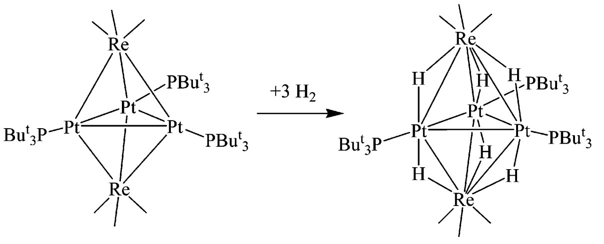

6 **7**

We have now investigated the reaction of $Pt(PBu^t_3)_2$ with $Re_3(CO)_{12}(\mu\text{-}H)_3$, **8**, and have obtained three new compounds: $PtRe_3(CO)_{12}(PBu^t_3)(\mu\text{-}H)_3$, **9**, $PtRe_2(CO)_9(PBu^t_3)(\mu\text{-}H)_2$, **10**, $Pt_2Re_2(CO)_7(PBu^t_3)_2(\mu\text{-}H)_2$, **11**. Compound **9** is a $Pt(PBu^t_3)$ adduct of **8**, but unlike the $Pt(PBu^t_3)$ adduct of its isoelectronic neighbor $Os_3(CO)_{12}$, the platinum atom from the $Pt(PBu^t_3)$ group in **9** has been inserted into the metal−metal bond to which it was added.[2] The unsaturated compound **11** adds H_2 reversibly to form the new compound $Pt_2Re_2(CO)_7(PBu^t_3)_2(\mu\text{-}H)_4$, **12**. Compound **12** adds CO to form the new open cluster compound $Pt_2Re_2(CO)_8(PBu^t_3)_2(\mu\text{-}H)_4$, **13**. The synthesis and characterizations of the new platinum−rhenium compounds **9**−**13** are reported here. A preliminary report of a portion of this work has been published.[8]

Experimental Section

General Data. Reagent grade solvents were dried by the standard procedures and were freshly distilled prior to use. Infrared spectra were recorded on a Thermo Nicolet Avatar 360 FT-IR spectrophotometer. ^1H NMR and $^{31}P\{^1H\}$ NMR were recorded on a Varian Mercury 400 spectrometer operating at 400.1 and 161.9 MHz, respectively. ^1H NMR and $^{31}P\{^1H\}$ NMR spectra of **11** and **12** were recorded on a Varian Inova 500 spectrometer operating at 500.2 and 202.5 MHz, respectively. $^{31}P\{^1H\}$ NMR spectra were externally referenced against 85% *ortho*-H_3PO_4. Electrospray mass spectrometric measurements were obtained on a MicroMass Q-Tof spectrometer. Elemental analyses were performed by Desert Analytics (Tucson, AZ). Bis(tri-*tert*-butyl phosphine)platinum(0), $Pt(PBu^t_3)_2$, was obtained from STREM and was used without further purification. $Re_3(CO)_{12}(\mu\text{-}H)_3$ was prepared according to the published procedure.[9] Product separations were performed by TLC in air on Analtech 0.25 and 0.5 mm silica gel 60 Å F_{254} glass plates.

Reaction of $Re_3(CO)_{12}(\mu\text{-}H)_3$ with $Pt(PBu^t_3)_2$ at Room Temperature. $Pt(PBu^t_3)_2$ (36.2 mg, 0.060 mmol) was added to a solution of $Re_3(CO)_{12}(\mu\text{-}H)_3$ (18.0 mg, 0.020 mmol) in 30 mL of CH_2Cl_2. The reaction mixture was stirred at room temperature for 14 h. The solvent was removed *in vacuo*, and the products were then isolated by TLC by using a 5:1 hexane/methylene chloride solvent mixture to yield in order of elution the following: 2.9 mg (14% yield) of yellow $PtRe_2(CO)_9(PBu^t_3)(\mu\text{-}H)_2$, **10**, and 5.1 mg (20% yield) of purple $PtRe_3(CO)_{12}(PBu^t_3)(\mu\text{-}H)_3$, **9**. Spectral data for **9**: IR ν_{CO} (cm^{-1} in hexane) 2104 (w), 2080 (m), 2046 (m), 2014 (vs), 2004 (s), 1989 (s), 1961 (m), 1949 (sh, w), 1935 (m); ^1H NMR (400 MHz, $CDCl_3$, rt, TMS) $\delta = 1.49$ (d, 27 H, CH_3, $^3J(P,H) = 13$ Hz), −9.17 (d, 2H, hydride, $^2J_P{-}H = 6$ Hz, $^1J_{Pt}{-}H = 756$ Hz), −11.39 (d, 1H, hydride, $^2J(P,H) = 9$ Hz, $^1J(Pt,H) = 118$ Hz); $^{31}P\{^1H\}$ NMR (162 MHz, $CDCl_3$, rt, 85% *ortho*-H_3PO_4) $\delta = 99.85$ (s, 1 P, $^1J(Pt,P) = 2856$ Hz). Mass Spec. ES$^+$/MS calcd for [M + CH_3CN + H], $[PtRe_3(CO)_{12}(PBu^t_3)(\mu\text{-}H)_3 + CH_3CN + H]^+$, 1338; found, 1338. Spectral data for **10**: IR ν_{CO} (cm^{-1} in hexane): 2101 (m), 2070 (s), 2008 (vs), 1991 (m), 1982 (m), 1972 (m), 1958 (s), 1950(m). ^1H NMR (400 MHz, $CDCl_3$, rt, TMS) $\delta = 1.53$ (d, $^3J(P,H) = 13$ Hz, 27 H, CH_3), −7.19 (d, $^2J(P,H) = 14$ Hz, $^1J(Pt, H) = 538$ Hz, 1H, hydride), −15.41 (s, $^2J(Pt, H) = 31$ Hz, 1H, hydride); $^{31}P\{^1H\}$ NMR (162 MHz, $CDCl_3$, rt, 85% *ortho*-H_3PO_4) $\delta = 110.6$ (s, $^1J(Pt,P) = 2936$ Hz, 1 P). Elemental analysis (%) calcd: 24.63, C; 2.76, H. Found: 25.31, C; 2.85, H.

Reaction of $Re_3(CO)_{12}(\mu\text{-}H)_3$ with $Pt(PBu^t_3)_2$ at 68 °C. $Pt(PBu^t_3)_2$ (30.0 mg, 0.050 mmol) and $Re_3(CO)_{12}(\mu\text{-}H)_3$ (23.0 mg, 0.026 mmol) were dissolved in 40 mL of hexane. After the mixture was heated to reflux for 2 h, the solvent was removed *in vacuo*, and the products were separated by TLC (silica gel) using a 3:1 hexane/methylene chloride solvent mixture. This yielded in order of elution the following: 9.2 mg (35% yield) of yellow $PtRe_2(CO)_9(PBu^t_3)(\mu\text{-}H)_2$, **10**, 1.8 mg (5% yield) of purple $PtRe_3(CO)_{12}(PBu^t_3)(\mu\text{-}H)_3$, **9**, and 8.4 mg (24% yield) of red $Pt_2Re_2(CO)_7(PBu^t_3)_2(\mu\text{-}H)_2$, **11**. Spectral data for **11**: IR ν_{CO} (cm^{-1} in CH_2Cl_2) 2035 (w), 2015 (m), 1994 (vs), 1916 (m, sh), 1900 (s, br). ^1H NMR (500 MHz, toluene-d_8, −40 °C, TMS) $\delta = 1.20$ (broad, 27 H, CH_3), −0.87 (s, 1H, hydride), −2.05 (dd, $^2J(P,H) = 6$ Hz, $^2J(P,H) = 11$ Hz, $^1J(Pt,H) = 621$ Hz, 1H, hydride). $^{31}P\{^1H\}$ NMR (202.5 MHz, toluene-d_8, −25 °C, 85% *ortho*-H_3PO_4): $\delta = 85.5$ (d, $^3J(P,P) = 82$ Hz, $^1J(Pt,P) = 3880$ Hz, 1 P), 112.7 (d, $^3J(P{-}P) = 82$ Hz, $^1J(Pt,P) = 2435$ Hz, 1 P). Mass Spec. ES$^+$/MS calcd for M$^+$, $[Pt_2Re_2(CO)_7(PBu^t_3)_2(\mu\text{-}H)_2]^+$, 1365; found, 1365. Elemental analysis (%) calcd: 27.27, C; 4.14, H. Found: 27.27, C; 3.90, H.

Reaction of 9 with PBu^t_3. An excess amount of PBu^t_3 (13 μL, 0.052 mmol) was added to a solution of **9** (7.0 mg, 0.005 mmol) in 15 mL of CH_2Cl_2. The reaction mixture was stirred at room temperature for approx 1.25 h during which time the purple colored solution turned

---

(5) (a) Xiao, J.; Puddephatt, R. J. *Coord. Chem. Rev.* **1995**, *143*, 457−500. (b) Augustine, S. M.; Sachtler, W. M. H. *J. Catal.* **1989**, *116*, 184−194. (c) Nacheff, M. S.; Kraus, L. S.; Ichikawa, M.; Hoffman, B. M.; Butt, J.; Sachtler, W. M. H. *J. Catal.* **1987**, *106*, 263−272.

(6) (a) Dyson, P. J.; McIndoe, J. S. *Angew. Chem., Int. Ed.* **2005**, *44*, 2. (b) Brayshaw, S. K.; Ingleson, M. J.; Green, J. C.; McIndoe, J. S.; Raithby, P. R.; Kociok-Köhn, G.; Weller, A. S. *J. Am. Chem. Soc.* **2006**, *128*, 6247−6263. (c) Brayshaw, S. K.; Ingleson, M. J.; Green, J. C.; Raithby, P. R.; Kociok-Köhn, G.; McIndoe, J. S.; Weller, A. S. *Angew. Chem., Int. Ed.* **2005**, *44*, 6875−6878. (d) Ingleson, M. J.; Mahon, M. F.; Raithby, P. R.; Weller, A. S. *J. Am. Chem. Soc.* **2004**, *126*, 4784−4785.

(7) (a) Adams, R. D.; Captain, B.; Beddie, C.; Hall, M. B. *J. Am. Chem. Soc.* **2007**, *129*, 986−1000. (b) Adams, R. D.; Captain, B. *Angew. Chem., Int. Ed.* **2005**, *44*, 2531−2533.

(8) Adams, R. D.; Captain, B.; Smith, M. D. *Angew. Chem., Int. Ed.* **2006**, *45*, 1109−1112.

(9) Kaesz, H. D.; Knox, S. A. R.; Koepke, J. W.; Saillant, R. B. *Chem. Commun.* **1971**, 477.

Table 1. Crystallographic Data for Compounds **9**−**11**

compound	**9**	**10**	**11**
empirical formula	$PtRe_3PO_{12}C_{24}H_{30}$	$PtRe_2PO_9C_{21}H_{29}$	$Pt_2Re_2P_2O_7C_{31}H_{54}$
formula weight	1295.14	1023.90	1363.26
crystal system	monoclinic	monoclinic	orthorhombic
lattice parameters			
a (Å)	9.0366(5)	27.395(3)	15.2359(14)
b (Å)	17.4393(9)	14.3333(16)	15.2464(14)
c (Å)	11.3378(6)	19.087(2)	50.847(5)
α (deg)	90	90	90
β (deg)	109.701(1)	130.348(2)	90.0
γ (deg)	90	90	90
V (Å^3)	1682.16(16)	5711.9(11)	11811.3(19)
space group	$P2_1/m$ (#11)	$C2/c$ (# 15)	$P2_12_12_1$ (#19)
Z value	2	8	12
ρ_{calcd} (g/cm^3)	2.560	2.38	2.30
μ (Mo Kα) (mm^{-1})	15.00	13.44	13.44
temperature (K)	296	294	100
$2\Theta_{max}$ (deg)	52.0	56.4	50.0
no. obsd ($I > 2\sigma(I)$)	2869	6066	17760
no. parameters	182	324	620
goodness of fit (GOF)[a]	1.062	1.024	1.056
max shift final cycle	0.000	0.002	0.002
Residuals*: R1; wR2	0.0400; 0.0864	0.0385; 0.0988	0.0734; 0.1747
absorption correction, max/min	multiscan 1.000/0.650	multiscan 1.000/0.473	multiscan 1.000/0.474
largest peak in final diff. map (e$^-$/Å^3)	1.47	2.27	10.17

[a] $R = \Sigma_{hkl}(||F_{obsd}| - |F_{calcd}||)/\Sigma_{hkl}|F_{obsd}|$; $R_w = [\Sigma_{hkl}w(|F_{obsd}| - |F_{calcd}|)^2/\Sigma_{hkl}wF_{obsd}{}^2]^{1/2}$, $w = 1/\sigma^2(F_{obsd})$; GOF $= [\Sigma_{hkl}w(|F_{obsd}| - |F_{calcd}|)^2/(n_{data} - n_{vari})]^{1/2}$.

Table 2. Crystallographic Data for Compounds 12−13

compound	**12**	**13**
empirical formula	$Pt_2Re_2P_2O_7C_{31}H_{56}\cdot{}^1/_2CH_2Cl_2$	$Pt_2Re_2P_2O_8C_{32}H_{58}$
formula weight	1409.76	1395.30
crystal system	monoclinic	triclinic
lattice parameters		
a (Å)	14.7121(9)	9.0728(4)
b (Å)	17.2332(11)	10.2568(5)
c (Å)	17.1146(11)	11.5861(6)
γ (deg)	90	95.204(1)
β (deg)	105.002(1)	97.889(1)
γ (deg)	90	101.259(1)
V (Å^3)	4191.3(5)	1039.73(9)
space group	$P2_1/c$ (#14)	$P\bar{1}$ (#2)
Z value	4	1
ρ_{calcd} (g/cm^3)	2.23	2.228
μ (Mo Kα) (mm^{-1})	12.59	12.627
temperature (K)	294	294
$2\Theta_{max}$ (deg)	56.6	56.6
no. obsd ($I > 2\sigma(I)$)	9236	4668
no. parameters	449	225
goodness of fit (GOF)[a]	1.001	1.078
max shift final cycle	0.000	0.001
residuals:[a] R1; wR2	0.0198; 0.0493	0.0200; 0.0497
absorption correction, max/min	multiscan 1.000/0.655	multiscan 1.000/0.621
largest peak in final diff map (e$^-$/Å^3)	0.97	0.614

[a] $R = \Sigma_{hkl}(||F_{obsd}| - |F_{calcd}||)/\Sigma_{hkl}|F_{obsd}|$; $R_w = [\Sigma_{hkl}w(|F_{obsd}| - |F_{calcd}|)^2/\Sigma_{hkl}wF_{obsd}{}^2]^{1/2}$, $w = 1/\sigma^2(F_{obsd})$; GOF $= [\Sigma_{hkl}w(|F_{obsd}| - |F_{calcd}|)^2/(n_{data} - n_{vari})]^{1/2}$.

light yellow/colorless. The solvent was removed *in vacuo*, and the product was then isolated by TLC by using pure CH_2Cl_2 solvent to yield 3.7 mg (76%) of colorless $Re_3(CO)_{12}(\mu\text{-}H)_3$.

Reaction of 10 with $Pt(PBu^t_3)_2$. $Pt(PBu^t_3)_2$ (30.0 mg, 0.050 mmol) was added to a solution of **10** (10.4 mg, 0.010 mmol) in 25 mL of hexane. The reaction mixture was heated to reflux for 8 h, after which the solvent was removed *in vacuo*. The products were separated by TLC (silica gel) using a 3:1 hexane/methylene chloride solvent mixture to yield in order of elution the following: 6.0 mg (58% yield) of starting yellow **10** and 3.0 mg (22% yield) of red $Pt_2Re_2(CO)_7(PBu^t_3)_2(\mu\text{-}H)_2$, **11**.

Addition of H_2 to 11. Compound **11** (16.1 mg, 0.012 mmol) was dissolved in 30 mL of heptane. With stirring, hydrogen gas was passed through the solution at room temperature for 12 h. The heptane solvent was then removed *in vacuo*, and the product was isolated by TLC (silica gel) using a 3:1 hexane/methylene chloride solvent mixture to yield 11.5 mg of bright-orange $Pt_2Re_2(CO)_7(PBu^t_3)_2(\mu\text{-}H)_4$, **12** (71% yield). Spectral data for **12**: IR ν_{CO} (cm^{-1} in hexane) 2041 (m), 2028 (s), 2006 (vs), 1936 (s), 1927 (vs), 1918 (m, sh). ^{1}H NMR (400 MHz, toluene-d_8, rt, TMS) $\delta = 1.29$ ppm (d, ^3J(P,H) = 13 Hz, 27 H, CH_3), 1.27 ppm (d, ^3J(P,H) = 13 Hz, 27 H, CH_3), −2.13 ppm (s, ^2J(Pt,H) = 37 Hz, 1H, hydride), −2.34 ppm (d, ^1J(Pt,H) = 588 Hz, ^2J(P,H) = 12 Hz, 1H, hydride), −6.10 ppm (dd, ^1J(Pt,H) = 801 Hz, ^2J(Pt,H) = 43 Hz, ^2J(P,H) = 10 Hz, ^3J(P,H) = 3 Hz, 2H, hydride). ^{31}P{^{1}H} NMR (162 MHz, toluene-d_8, 25 °C, 85% *ortho*-H_3PO_4) 95.75 ppm (d, ^3J(P,P) = 62 Hz, ^1J(Pt,P) = 3388 Hz, ^2J(Pt,P) = 197 Hz, 1P), 108.14 ppm (d, ^3J(P,P) = 62 Hz, ^1J(Pt,P) = 2720 Hz, ^2J(Pt,P) = 296 Hz, 1P). Mass Spec. ES$^+$/MS calcd for M$^+$, $[Pt_2Re_2(CO)_7(PBu^t_3)_2(\mu\text{-}H)_4]^+$, 1367; found, 1367. Elemental analysis (%) calcd: 27.23, C; 4.28, H. Found: 27.64, C; 3.99, H.

Controlled Addition of CO to 12. Compound **12** (13.5 mg, 0.010 mmol) was dissolved in 7 mL of heptane in a 10 mL Schlenk tube. The Schlenk tube was then evacuated and filled with nitrogen three times and finally evacuated partially on the last filling. Carbon monoxide gas (CO) (215 μL, 0.009 mmol) was added to the partially evacuated Schlenk tube by using a syringe. The reaction was stirred at room temperature for 2 h. The solvent was then removed *in vacuo*, and the product was isolated by TLC (silica gel) using a 4:1 hexane/methylene chloride solvent mixture to yield 10.0 mg (73% yield) of pink $Pt_2Re_2(CO)_8(PBu^t_3)_2(\mu\text{-}H)_4$, **13**, and 2.1 mg of unreacted **12**. Spectral data for **13**: IR ν_{CO} (cm^{-1} in hexane) 2083 (vw), 2062 (m), 2028 (vw), 1993 (m), 1974 (s), 1934 (s), 1903 (vw). ^{1}H NMR (400 MHz, toluene-d_8, rt, TMS) $\delta = 1.34$ ppm (d, ^3J(P,H) = 12 Hz, 54 H, CH_3), −6.27 ppm (t, ^1J(Pt,H) = 683 Hz, ^2J(P,H) = 7 Hz, 2H, hydride). ^{31}P{^{1}H} NMR (162 MHz, toluene-d_8, rt, 85% *ortho*-H_3PO_4): 98.9 ppm (s, ^3J(P,P) = 301 Hz, ^1J(Pt,P) = 2554 Hz, ^2J(Pt,P) = 2253 Hz, 1P). Mass Spec. ES$^+$/MS calcd for M$^+$, $[Pt_2Re_2(CO)_8(PBu^t_3)_2(\mu\text{-}H)_4]^+$, 1395; found, 1395. NOTE: When CO gas was bubbled though a solution of **12** in hexane, the color changed from orange to yellow within 1 min. An IR spectrum of the reaction mixture indicated formation of compound **10** and $Pt_3(PBu^t_3)_3(CO)_3$.[10]

Reaction of 11 with $Pt(PBu^t_3)_2$. $Pt(PBu^t_3)_2$ (5.1 mg, 0.0085 mmol) and **11** (6.1 mg, 0.0045 mmol) in 10 mL of octane were refluxed for 1.5 h. An IR spectrum of the reaction mixture at this time showed almost complete conversion to $Pt_3Re_2(CO)_6(PBu^t_3)_3(\mu\text{-}H)_2$, **14**. Due to the instability of **14**,[7a] this compound was not isolated in this work.

Reaction of 12 with $Pt(PBu^t_3)_2$. $Pt(PBu^t_3)_2$ (6.5 mg, 0.011 mmol) and **12** (7.5 mg, 0.0055 mmol) were dissolved in 15 mL of heptane. After the mixture heated to reflux for 20 min, the solvent was removed *in vacuo*, and the products were separated by TLC (silica gel) using a 4:1 hexane/methylene chloride solvent mixture. This yielded in order of elution the following: a trace amount of yellow $PtRe_2(CO)_9(PBu^t_3)(\mu\text{-}H)_2$, **10**, a trace amount of pink **13**, 6.2 mg (65% yield) of brown $Pt_3Re_2(CO)_6(PBu^t_3)_3(\mu\text{-}H)_4$, **15**, 0.9 mg of unreacted **12**, and 1.0 mg (13% yield) of **11**.

Thermal Elimination of Hydrogen from 12 at 97 °C. Compound **12** (12.8 mg, 0.009 mmol) was dissolved in 60 mL of heptane in a 100 mL three-neck flask equipped with a reflux condenser and a gas inlet. A slow stream of nitrogen (flow rate ~27 mL/min) was allowed to flow through the flask while refluxing this solution for 4 h. The progress of this reaction can be monitored by IR. The heptane solvent was then removed *in vacuo*, and the products were separated by TLC (silica gel) using a 3:1 hexane/methylene chloride solvent mixture to yield in

---

[10] Goel, R. G.; Ogini, W. O.; Srivastava, R. C. *J. Organomet. Chem.* **1981**, *214*, 405−417.

order of elution the following: 0.7 mg (5% yield) of starting orange $Pt_2Re_2(CO)_7(PBu^t{}_3)_2(\mu\text{-}H)_4$, **12**, and 11.5 mg (90% yield) of red $Pt_2Re_2(CO)_7(PBu^t{}_3)_2(\mu\text{-}H)_2$, **11**.

Photoelimination of Hydrogen from 12. Compound **12** (12.8 mg, 0.009 mmol) was dissolved in 60 mL of hexane in a 100 mL three-neck flask equipped with a reflux condenser and a gas inlet. A slow stream of nitrogen (flow rate ~27 mL/min) was allowed to flow through the flask while irradiating this solution for 4 h using a medium-pressure mercury UV lamp (1000 W). The progress of this reaction can be monitored by IR. The hexane solvent was then removed *in vacuo*, and the products were separated by TLC (silica gel) using a 3:1 hexane/methylene chloride solvent mixture to yield in order of elution the following: trace amounts (<0.5 mg) of pink $Pt_2Re_2(CO)_8(PBu^t{}_3)_2(\mu\text{-}H)_4$, **13**, trace amounts (<0.5 mg) of orange $Pt_3Re_2(CO)_6(PBu^t{}_3)_3(\mu\text{-}H)_6$, **7**, trace amounts (<0.5 mg) of brown **15**, 1.0 mg (8% yield) of starting orange **12**, and 10.6 mg (83% yield) of red **11**.

Detection of Hydrogen Elimination by ^{1}H NMR. A 6.0 mg amount of **12** was dissolved in 0.6 mL of toluene-d_8 in a 5 mm NMR tube. The NMR tube was evacuated and filled with nitrogen five times. The NMR tube was then evacuated partially. The partially evacuated NMR tube was placed in an oil bath maintained at 100 °C for 3 h. After this period of time the NMR tube was taken out of the oil bath and kept cold (ice−water bath) while proceeding to acquire the ^{1}H NMR spectrum. The ^{1}H NMR spectrum of this solution showed a singlet at $\delta = 4.51$ indicating the presence of H_2 in solution. Similarly, H_2 was also detected by irradiating a sample of **12** in toluene-d_8 solvent in an NMR tube for 4 h using a medium-pressure mercury UV lamp (1000 W).

Determination of the Kinetic Isotope Effect (KIE) for the Addition of H_2 to 11. In a 100 mL Schlenk flask, 10.0 mg of **11** in 40 mL of hexane were stirred overnight at room temperature to ensure that **11** had completely dissolved. The flask was then evacuated and filled with deuterium gas three times. The flask was stirred at room temperature under the deuterium atmosphere. During this time, samples were removed periodically via syringe, and IR spectra in the CO region were recorded. Under identical conditions, 10.0 mg of **11** in 40 mL of hexane were stirred at room temperature under a hydrogen atmosphere, and IR spectra were recorded periodically. At certain times the IR spectra of the two samples appeared to be virtually the same. The KIE was determined to be the ratio of the reaction times D/H for the two reactions when the spectra appeared to be identical. For example, the IR spectrum for the D_2 addition reaction after 2.25 h was approximately the same as the IR spectrum after 1.5 h for the H_2 addition reaction, thus the D_2/H_2 isotope effect was determined to be 1.5(1).

Crystallographic Analyses. Single crystals of **9**, **10**, **11**, **12**, and **13** suitable for X-ray diffractions were obtained by slow evaporation of solvent from solutions in methylene chloride/hexane solvent mixtures at −20 °C. Each data crystal was glued onto the end of a thin glass fiber. X-ray intensity data were measured by using a Bruker SMART APEX CCD-based diffractometer using Mo Kα radiation ($\lambda = 0.710\ 73$ Å). The raw data frames were integrated with the SAINT+ program by using a narrow-frame integration algorithm.[11] Correction for Lorentz and polarization effects were also applied with SAINT+. An empirical absorption correction based on the multiple measurement of equivalent reflections was applied using the program SADABS. All structures were solved by a combination of direct methods and difference Fourier syntheses and refined by full-matrix least-squares on F^2, using the SHELXTL software package.[12] All non-hydrogen atoms were refined with anisotropic thermal parameters. Hydrogen atoms were placed in geometrically idealized positions and included as standard riding atoms during the least-squares refinements. Crystal data, data collection parameters, and results of the refinements are listed in Tables 1 and 2.

The crystals of compound **9** belong to the monoclinic crystal system. The systematic absences in the intensity data for these crystals were consistent with either of the space groups $P2_1$ and $P2_1/m$. The structure could be solved only in the latter space group. The three hydrido ligands were located but could not be refined and were included finally as fixed contributions where they were located in the diff. Fourier maps. The quaternary carbons on the tri-*tert*-butyl phosphine ligand were disordered over two orientations and were refined in the ratio 50/50. The carbon atoms of the tri-*tert*-butyl phosphine ligand were refined with isotropic displacement parameters.

For compound **10** the systematic absences in the data indicated two possible space groups, $C2/c$ or Cc. The former was attempted first and confirmed by the successful solution and refinement of the structure. The two hydrido ligands were located and refined successfully with isotropic thermal parameters.

Compound **11** crystallized in the orthorhombic crystal system. The space group $P2_1P2_1P2_1$ was identified on the basis of the patterns of systematic absences in the data. The compound crystallizes with three independent molecules in the crystallographic asymmetric unit. The structure is disordered. The disorder is evident from the presence of several large residual electron density peaks in the vicinity of the metal atoms. Various twinning and disorder models were attempted but were unsuccessful. Careful examination of the diffraction pattern showed no indication of a different unit cell. Several attempts were made to crystallize this compound from different solvent mixtures and different crystallization conditions; however, beautiful pristine looking red single crystals were always obtained with the same unit cell dimensions. Only the platinum, rhenium, and phosphorus atoms were refined with anisotropic thermal parameters. The two hydrido ligands could not be located.

Compound **12** crystallized in the monoclinic crystal system. The space group $P2_1/c$ was identified on the basis of the patterns of systematic absences in the data. Each of the four hydrido ligands were located and refined successfully with isotropic thermal parameters. One-half of a molecule of methylene chloride from the crystallization solvent cocrystallized with the complex. The solvent molecule was included in the analysis and was satisfactorily refined with anisotropic thermal parameters.

Compound **13** crystallized in the triclinic crystal system. The space group $P\bar{1}$ was assumed and confirmed by the successful refinement and solution of the structure. With $Z = 1$, the molecule is crystallographically centrosymmetrical and thus contains only one-half of the formula equivalent of the molecule in the asymmetric crystal unit. Both independent hydrido ligands were located and refined successfully with isotropic thermal parameters.

Details of the Computational Treatments. All calculations were performed using the Gaussian 03 suite of programs.[13] The computational model of the experimental system was constructed with PMe_3 ligands in place of $P(t\text{-}Bu)_3$ ligands to reduce the computational demands of the system. Optimized gas-phase geometries were obtained by using the B3PW91 DFT method.[14,15] The basis set (BS1) used for geometry optimizations and energy calculations was implemented as follows: for rhenium and platinum, the valence double-ζ LANL2DZ[16] basis sets

---

(11) *SAINT+*, version 6.2a; Bruker Analytical X-ray System, Inc.: Madison, Wisconsin, U.S.A., 2001.

(12) Sheldrick, G. M. *SHELXTL*, version 6.1; Bruker Analytical X-ray Systems, Inc.: Madison, Wisconsin, U.S.A., 1997.

(13) All calculations were conducted using the Gaussian03 suite of programs: Frisch, M. J., et al. *Gaussian 03*, revision B.4; Gaussian, Inc.: Pittsburgh, PA, 2003.

(14) Becke, A. D. *J. Chem. Phys.* **1993**, *98*, 5648−5652.

(15) (a) Burke, K.; Perdew, J. P.; Wang, Y. In *Electronic Density Functional Theory: Recent Progress and New Directions*; Dobson, J. F., Vignale, G., Das, M. P., Eds.; Plenum: New York, 1998; pp 81−111. (b) Perdew, J. P. In *Electronic Structure of Solids '91*; Ziesche, P., Eschrig, H., Eds.; Akademie Verlag: Berlin, 1991; p 11. (c) Perdew, J. P.; Chevary, J. A.; Vosko, S. H.; Jackson, K. A.; Pederson, M. R.; Singh, D. J.; Fiolhais, C. *Phys. Rev. B* **1992**, *46*, 6671−6687. (d) Perdew, J. P.; Chevary, J. A.; Vosko, S. H.; Jackson, K. A.; Pederson, M. R.; Singh, D. J.; Fiolhais, C. *Phys. Rev. B* **1993**, *48*, 4978. (e) Perdew, J. P.; Burke, K.; Wang, Y. *Phys. Rev. B* **1996**, *54*, 16533−16539.

(16) (a) Hay, P. J.; Wadt, W. R. *J. Chem. Phys.* **1985**, *82*, 270−283. (b) Wadt, W. R.; Hay, P. J. *J. Chem. Phys.* **1985**, *82*, 284−298. (c) Hay, P. J.; Wadt, W. R. *J. Chem. Phys.* **1985**, *82*, 299−310.

were supplemented with sets of 6p functions for transition metals developed by Couty and Hall;[17] for phosphorus, the LANL2DZdp basis set was used;[16,18,19] for carbon and oxygen, the 6-31G(d′)[20] basis sets were used; for the hydrogen atoms attached to carbon, the 6-31G basis set was used;[20] while, for dihydrogen and for the hydrogen atoms that bonded to the platinum and rhenium, the 6-31G++(d′,p′) basis set was used.[20] All structures were calculated in singlet spin states using the restricted B3PW91 method. Calculating the harmonic vibrational frequencies and noting the number of imaginary frequencies confirmed the nature of all intermediates (NImag = 0) and transition state structures (NImag = 1).

Fenske−Hall Molecular Orbital Calculations. A single-point molecular orbital calculation on **11** was performed on the molecular structure as derived from the single-crystal X-ray diffraction analysis. PH_3 was used in place of PBu^t_3 in these calculations. The two hydride ligands were calculated using the program XHYDEX in the WINGX suit of programs.[21] The molecular orbital calculations reported herein were performed by using the Fenske−Hall method.[22] Contracted double-ζ basis sets were used for the Re 5d, Pt 5d, P 3p, and C and O 2p atomic orbitals. The Fenske−Hall molecular orbital method is an approximate self-consistent-field (SCF) nonempirical method that is capable of calculating molecular orbitals for very large transition metal systems and has built-in fragment analysis routines that allow one to assemble transition metal cluster structures from the ligand-containing fragments.

Results and Discussion

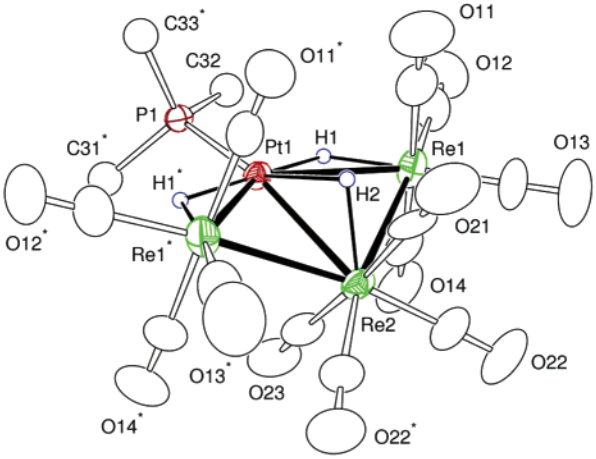

Figure 1. An ORTEP diagram of the molecular structure of $PtRe_3(CO)_{12}(PBu^t_3)(\mu\text{-}H)_3$, **9**, showing 40% probability thermal ellipsoids. Selected interatomic distances (Å) and angles (deg) are as follows: Pt(1)−Re(1) = 2.9280(5); Pt(1)−Re(2) = 2.9532(7); Pt(1)−P(1) = 2.312(3); Re(1)−Re(2) = 3.0476(5); Re(1)−Pt(1)−Re(1*) = 119.41(2); Re(1)−Pt(1)−Re(2) = 62.420(12).

Two new compounds $PtRe_3(CO)_{12}(PBu^t_3)(\mu\text{-}H)_3$, **9**, and $PtRe_2(CO)_9(PBu^t_3)(\mu\text{-}H)_2$, **10**, were obtained from the reaction of $Pt(PBu^t_3)_2$ with $Re_3(CO)_{12}(\mu\text{-}H_3)$, **8**, at room temperature in the yields 20% and 14%, respectively. Both products were characterized by IR, ^1H and ^{31}P NMR, single-crystal X-ray diffraction, and elemental analyses. An ORTEP diagram of the molecular structure of **9** is shown in Figure 1. The compound consists of a butterfly tetrahedral cluster of four metal atoms, three of rhenium and one of platinum. In the solid state, the molecular structure of compound **9** contains reflection symmetry in the crystal with the platinum atom, the rhenium atom Re(2), and the phosphorus atom of the phosphine ligand lying on the reflection plane. There are 12 carbonyl ligands, four terminal COs on each rhenium atom. The platinum atom is bonded to all three rhenium atoms: Pt(1)−Re(1) = Pt(1)−Re(1*) = 2.9280(5) Å, Pt(1)−Re(2) = 2.9532(7) Å. The two equivalent Re−Re distances Re(1)−Re(2) = Re(1*)−Re(2) = 3.0476(5) Å are not significantly different from the Re−Re distance in $Re_2(CO)_{10}$ [3.042(1) Å][23] but are significantly shorter than the hydride bridged Re−Re distances, 3.241(2) Å, found in **8**.[24] Hydride bridged metal−metal bonds are usually longer than the corresponding bonds that do not have bridging hydride ligands.[25]

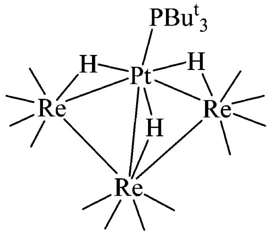

9

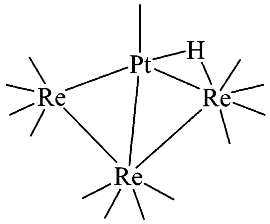

16

The metal cluster is structurally similar to the platinum−rhenium dianion, $[PtRe_3(CO)_{13}(\mu\text{-}H)]^{2-}$, **16**, obtained by Beringhelli et al. from the reaction of $[\{Pt_3(CO)_6\}_n]^{2-}$ with $[Re_2(CO)_8H_2(\mu\text{-}H)]^-$.[26] The hydride bridged Pt−Re bond in **16** is 2.799(1) Å in length. The Pt−Re bonds in **16** that do not have bridging hydride ligands are 2.706(1) Å and 2.798(2) Å. The Re−Re distances in **16** are 3.046(1) Å and 3.091(1) Å. Compound **9** contains one PBu^t_3 ligand that is coordinated to the platinum atom, Pt(1)−P(1) = 2.312(3) Å. There are three hydrido ligands. They were located in the structural analysis but were not refined. One bridges each of the three Pt−Re bonds. They appear only as two resonances in a 2/1 ratio in the ^1H NMR spectrum, $\delta = -9.17$ (d, 2H, hydride, $^2J_P{-}H = 6$ Hz, $^1J_{Pt}{-}H = 756$ Hz), −11.39 (d, 1H, hydride, $^2J(P,H) = 9$ Hz, $^1J(Pt,H) = 118$ Hz), because two of them are equivalent. Both resonances show one bond coupling to platinum. Two bond

---

(17) Couty, M.; Hall, M. B. *J. Comput. Chem.* **1996**, *17*, 1359−1370.

(18) Basis sets were obtained from the Extensible Computational Chemistry Environment Basis Set Database, Version 02/25/04, as developed and distributed by the Molecular Science Computing Facility, Environmental and Molecular Sciences Laboratory which is part of the Pacific Northwest Laboratory, P.O. Box 999, Richland, Washington 99352, U.S.A., and funded by the U.S. Department of Energy. The Pacific Northwest Laboratory is a multiprogram laboratory operated by Battelle Memorial Institute for the U.S. Department of Energy under Contract DE-AC06−76RLO 1830. Contact Karen Schuchardt for further information.

(19) Check, C. E.; Faust, T. O.; Bailey, J. M.; Wright, B. J.; Gilbert, T. M.; Sunderlin, L. S.; *J. Phys. Chem. A* **2001**, *105*, 8111−8116.

(20) (a) Ditchfield, R.; Hehre, W. J.; Pople, J. A. *J. Chem. Phys.* **1971**, *54*, 724−728. (b) Hehre, W. J.; Ditchfield, R.; Pople, J. A. *J. Chem. Phys.* **1972**, *56*, 2257−2261. (c) Hariharan, P. C.; Pople, J. A. *Theor. Chim. Acta* **1973**, *28*, 213−222. (d) Petersson, G. A.; Al-Laham, M. A. *J. Chem. Phys.* **1991**, *94*, 6081−6090. (e) Petersson, G. A.; Bennett, A.; Tensfeldt, T. G.; Al-Laham, M. A.; Shirley, W. A.; Mantzaris, J. *J. Chem. Phys.* **1988**, *89*, 2193−2218. (f) Foresman, J. B.; Frisch, Æ. *Exploring Chemistry with Electronic Structure Methods*, 2nd ed.; Gaussian, Inc.: Pittsburgh, PA; p 110. The 6-31G(d′,p′) basis set has the d polarization functions for C, N, O, and F taken from the 6-311G(d) basis set, instead of those which use the exponent with an original arbitrarily assigned value of 0.8 used in the 6-31G(d) basis set.

(21) Farrugia, L. J. *J. Appl. Crystallogr.* **1999**, *32*, 837−838. http://www.chem.gla.ac.uk/~louis/wingx.

(22) Hall, M. B.; Fenske, R. F. *Inorg. Chem.* **1972**, *11*, 768−779; Manson, J.; Webster, C. E.; Perez, L. M.; Hall, M. B. http://www.chem.tamu.edu/jimp2/index.html.

(23) Churchill, M. R.; Amoh, K. N.; Wasserman, H. J. *Inorg. Chem.* **1981**, *20*, 1609−1611.

(24) Masciocchi, N.; Sironi, A.; D'Alfonso, G. *J. Am. Chem. Soc.* **1990**, *112*, 9395−9397.

(25) (a) Bau, R.; Drabnis, M. H. *Inorg. Chim. Acta* **1997**, *259*, 27−50. (b) Teller, R. G.; Bau, R. *Struct. Bonding (Berlin)* **1981**, *41*, 1−82.

Table 3. Selected Intramolecular Distances and Angles for **11**[a]

molecule 1			molecule 2			molecule 3		
atom	atom	distance (Å)	atom	atom	distance (Å)	atom	atom	distance (Å)
Pt(1)	Pt(2)	2.6665(16)	Pt(3)	Pt(4)	2.6738(16)	Pt(5)	Pt(6)	2.6646(17)
Pt(1)	Re(1)	2.9100(15)	Pt(3)	Re(3)	2.9152(16)	Pt(5)	Re(5)	2.8972(18)
Pt(1)	Re(2)	2.8648(16)	Pt(3)	Re(4)	2.8662(15)	Pt(5)	Re(6)	2.8674(18)
Pt(2)	Re(1)	2.7259(15)	Pt(4)	Re(3)	2.7019(16)	Pt(6)	Re(5)	2.7116(18)
Pt(2)	Re(2)	2.6119(15)	Pt(4)	Re(4)	2.6144(15)	Pt(6)	Re(6)	2.6139(18)
Re(1)	Re(2)	2.9419(13)	Re(3)	Re(4)	2.9388(14)	Re(5)	Re(6)	2.921(2)

[a] Estimated standard deviations in the least significant figure are given in parentheses.

couplings to platinum are usually less than 40 Hz.[27] Overall, compound **9** has only 60 valence electrons; two less than the amount 62 usually found for butterfly tetrahedral cluster complexes. This can be explained by the presence of the platinum atom that formally has only 16 valence electrons.

We showed previously that the reaction of $\mathrm{Os_3(CO)_{12}}$, which is isoelectronic with **8**, with $\mathrm{Pt(PBu^t_3)_2}$ resulted in the formation of $\mathrm{PPBu^t_3}$ adducts of $\mathrm{Os_3(CO)_{12}}$, $\mathrm{Os_3(CO)_{12}[Pt(PBu^t_3)]_{\mathit{n}}}$ $n = 1-3$ by the addition of $\mathrm{Pt(PBu^t_3)}$ groups across the Os−Os bonds.[2] There was no evidence for insertion of the $\mathrm{Pt(PBu^t_3)}$ group into the metal−metal bond in these additions. In the reaction of **8** with $\mathrm{Pt(PBu^t_3)_2}$, only one $\mathrm{Pt(PBu^t_3)}$ group was added to the molecule of **8**, and it was inserted into the Re−Re bond.

Since there was no loss of CO from the **8** in the formation of **9**, compound **9** could be viewed as a $\mathrm{Pt(PBu^t_3)}$ adduct of **8** formed by the insertion of the platinum atom from a $\mathrm{Pt(PBu^t_3)}$ group into one of the hydride bridged metal−metal bonds. Two of the hydrido ligands then migrated from Re−Re bonds to the new Pt−Re bonds. These results demonstrate an interesting new feature of the reactions of $\mathrm{Pt(PBu^t_3)_2}$, namely that the $\mathrm{Pt(PBu^t_3)}$ group derived from it can actually be cleanly inserted into a hydride bridged rhenium−rhenium bond without loss of a CO ligand.

Interestingly, when **9** was treated with $\mathrm{PBu^t_3}$, it was converted back to **8** in 76% yield. The conversion of **9** back to **8** demonstrates that the insertion of the $\mathrm{Pt(PBu^t_3)}$ group into the hydride bridged Re−Re bond is reversible.

An ORTEP diagram of the molecular structure of **10** is shown in Figure 2. This compound contains a triangular cluster of three metal atoms, two of rhenium and one of platinum. There are nine carbonyl ligands, four terminal COs on each rhenium atom and one on the platinum atom. Compound **10** contains two hydrido ligands that were located and refined in the structural analysis. One bridges the Pt(1)−Re(1) bond, and the other bridges the Re−Re bond, Re(1)−Re(2) = 3.1726(4) Å. As expected, the hydride bridged Pt−Re bond, Pt(1)−Re(1) = 2.9667(4) Å, is significantly longer than the unbridged Pt−Re bond, Pt(1)−Re(2) = 2.8133(4) Å. The two highly shielded resonances in the ^{1}H NMR spectrum, $\delta = -7.19$ (d, ^2J(P,H) = 14 Hz, ^1J(Pt, H) = 538 Hz) and -15.41 (s, ^2J(Pt, H) = 31 Hz), are attributed to the hydrido ligands. Compound **10** contains one $\mathrm{PBu^t_3}$ ligand that is coordinated to the platinum atom, Pt(1)−P(1) 2.3837(15) Å. Compound **10** is structurally similar to the platinum−rhenium compound $\mathrm{PtRe_2(CO)_9(PPh_3)_2(\mu\text{-}H)_2}$, **17**, obtained by Beringhelli et al. from the reaction of $\mathrm{Re_2(CO)_8(\mu\text{-}H)_2}$ with $\mathrm{Pt(PPh_3)_2(C_2H_4)}$.[26] The hydride-bridged Pt−Re bond in **17** is 2.906(1) Å in length; the Pt−Re bond without a hydride bridge is 2.788(1) Å. The hydride-bridged Re−Re length in **17** is 3.203(1) Å. Compound **10** has only 46 valence electrons; two less than the 48 amount expected for electron precise triangular metal cluster complexes. As in **9**, this can be explained by a 16 electron configuration at the platinum atom.

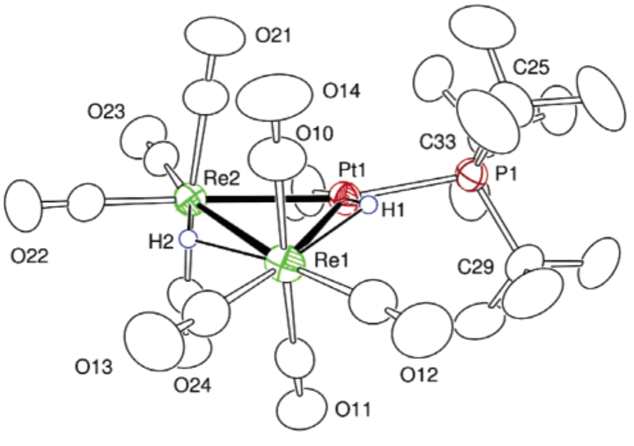

Figure 2. An ORTEP diagram of the molecular structure of $\mathrm{PtRe_2(CO)_9(PBu^t_3)(\mu\text{-}H)_2}$, **10**, showing 40% probability thermal ellipsoids. Selected interatomic distances (Å) and angles (deg) are as follows: Pt(1)−P(1) 2.3837(15), Pt(1)−Re(2) = 2.8133(4), Pt(1)−Re(1) = 2.9667(4), Pt(1)−H(1) = 1.87(6), Re(1)−Re(2) = 3.1726(4), Re(1)−H(1) = 1.89(6), Re(1)−H(2) = 1.85(12), Re(2)−H(2) = 1.87(12); Re(2)−Pt(1)−Re(1) = 66.52(1), Pt(1)−Re(1)−Re(2) = 54.424(10), Pt(1)−Re(2)−Re(1) = 59.056(8).

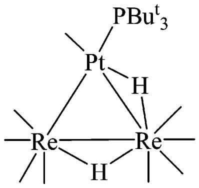

10

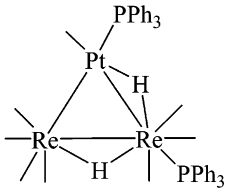

17

When the reaction of **8** with of $\mathrm{Pt(PBu^t_3)_2}$ was performed in hexane at reflux, the new compound $\mathrm{Pt_2Re_2(CO)_7(PBu^t_3)_2(\mu\text{-}H)_2}$, **11**, was obtained in 24% yield in addition to smaller quantities of **9** (5%) and an increased quantity of **10** (35%). It was subsequently shown that **11** is formed from **10** in 58% yield by reaction with $\mathrm{Pt(PBu^t_3)_2}$ for 8 h at hexane reflux.

Compound **11** crystallizes with three independent molecules in the crystallographic asymmetric unit. All three molecules are structurally similar. An ORTEP diagram of the molecular structure of one of the three molecules of **11** is shown in Figure 3. Selected bond distances for the three molecules are listed in Table 3. This compound consists of a cluster of four metal

---

(26) Beringhelli, T.; Ceriotti, A.; Ciani, G.; D'Alfonso, G.; Garlaschelli, L.; Della Pergola, R.; Moret, M.; Sironi, A. *J. Chem. Soc., Dalton Trans.* **1993**, 199−200.

(27) Adams, R. D.; Pompeo, M. P.; Wu, W. *Inorg. Chem.* **1991**, *30*, 2425−2432.

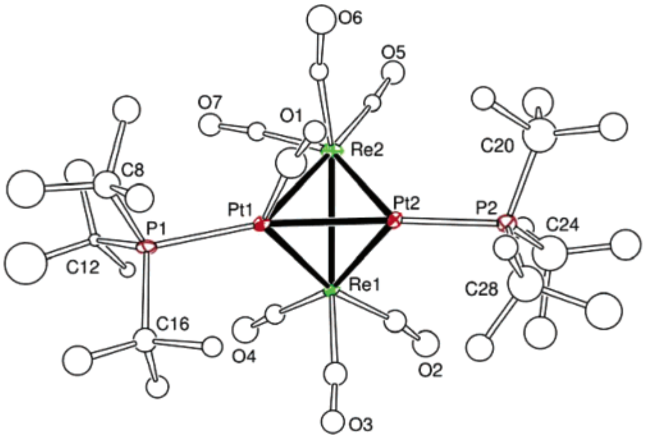

Figure 3. An ORTEP diagram of the molecular structure of one of the three independent molecules in the unit cell of the crystal of $Pt_2Re_2(CO)_7(PBu^t{}_3)_2(\mu\text{-}H)_2$, **11**, showing 40% probability thermal ellipsoids.

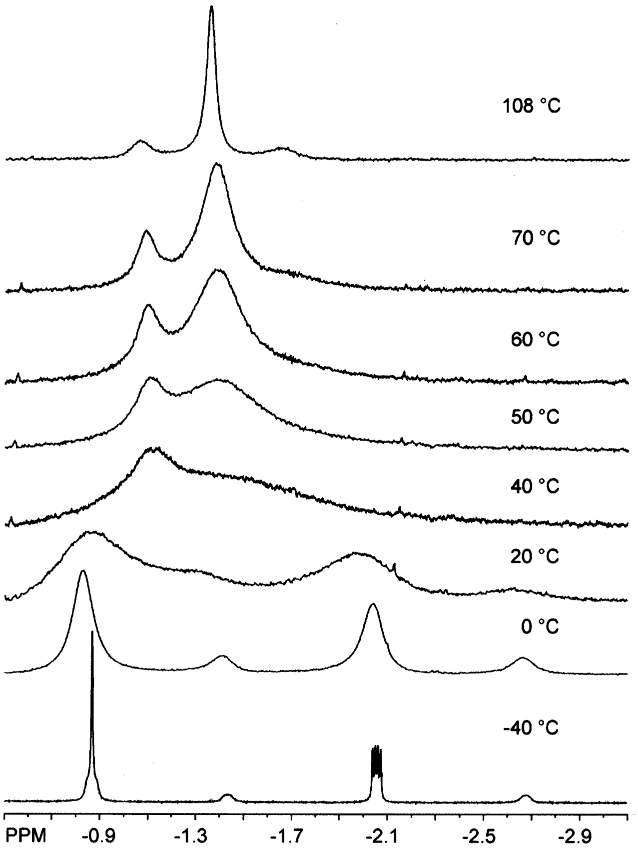

Figure 4. ^{1}H NMR spectra at 500 MHz of compound **11** at various temperatures in toluene-d_8 solvent.

atoms, two of rhenium and two of platinum, in the shape of a tetrahedron. The molecule contains seven carbonyl ligands. Three are located on each rhenium atom, and one is on one of the two platinum atoms; see Pt(1) in Figure 3. Each platinum atom contains one $PBu^t{}_3$ ligand. Compound **11** contains only 54 cluster valence electrons. This is six less than the 60 required for a tetrahedral cluster in which all metal atoms have 18 electron configurations; see below. The platinum atom Pt(2) has one less ligand than Pt(1). This could imply some electron unsaturation at this atom. The two Pt−Re bonds to Pt(2), Pt(2)−Re(1) = 2.7259(15) [2.7019(16) Å, 2.7116(18) Å] and Pt(2)−Re(2) = 2.6119(15) Å [2.6144(15)Å, 2.6139(18) Å], are much shorter than the unbridged Pt−Re bond in **10**, 2.8133(4) Å. The Pt−Pt bond is short but not unusually short, 2.6665(16) Å [2.6738(16) Å and 2.6646(17) Å]. The molecular formula as confirmed from the parent ion in its mass spectrum indicates the presence of two hydrido ligands. This is supported by the ^{1}H NMR spectrum recorded at −40 °C, which shows two highly shielded resonances at $\delta = -0.87$ (s, 1H), −2.05 (dd, $^2J(P,H) = 6$ Hz, $^2J(P,H) = 11$ Hz, $^1J(Pt,H) = 621$ Hz, 1H). Due to minor disorder the structural analysis was not high and therefore the hydrido ligands could not be located. The absence of ^{31}P−H and ^{195}Pt−H couplings to the resonance at −0.87 ppm suggests that this hydrido ligand probably bridges the Re−Re bond. The resonance at −2.05 ppm exhibits one bond coupling to one Pt atom, $^1J(Pt,H) = 621$ Hz, and small couplings to both phosphorus atoms, $^2J(P,H) = 6$ Hz and $^2J(P,H) = 11$ Hz). This could be consistent with a number of locations about the cluster, but molecular orbital calculations described below strongly indicate that it bridges the Pt(1)−Re(1) bond shown in Figure 3. This is also supported by the long length of the Pt(1)−Re(1) bond, Pt(1)−Re(1) = 2.9100(15) Å.[25]

The hydrido ligands in **11** are dynamically active on the NMR time scale as shown in the variable temperature ^{1}H NMR spectra presented in Figure 4. Since ^{195}Pt coupling to the hydride resonance is observed in the dynamically averaged spectrum at 108 °C, the exchange mechanism must be an intramolecular one. The most plausible mechanism for the interchange of the hydrido ligands is by migratory shifts from one edge of the cluster to another until site interchange is completed.[28]

The $^{31}P\{^1H\}$ NMR at −25 °C exhibits two resonances of equal intensity with mutual couplings and couplings to ^{195}Pt, $\delta = 85.5$ (d, 1 P, $^3J_{P}-P = 82$ Hz, $^1J_{Pt}-P = 3880$ Hz), 112.7 (d, 1 P, $^3J_{P}-P = 82$ Hz, $^1J_{Pt}-P = 2435$ Hz). This is consistent with the structure as found in the solid state. The resonances broaden and average as the temperature is raised, although the fast exchange limit could not be obtained due to the onset of decomposition of the compound at temperatures greater than 100 °C. This is indicative of yet another dynamical process whereby the environments of the phosphine ligands are interchanged. The most simple mechanism for this would be a simple shifting of the terminal CO ligand on atom Pt(1) to an equivalent position on atom Pt(2). This shift will probably involve traversing an intermediate in which the CO ligand is simultaneously bonded to both Pt atoms; see Scheme 1. Bridge-terminal

Scheme 1

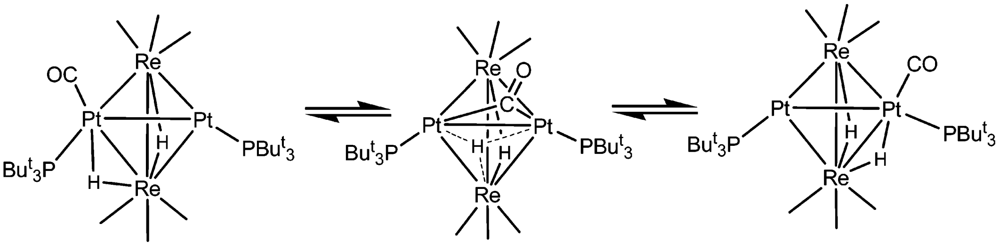

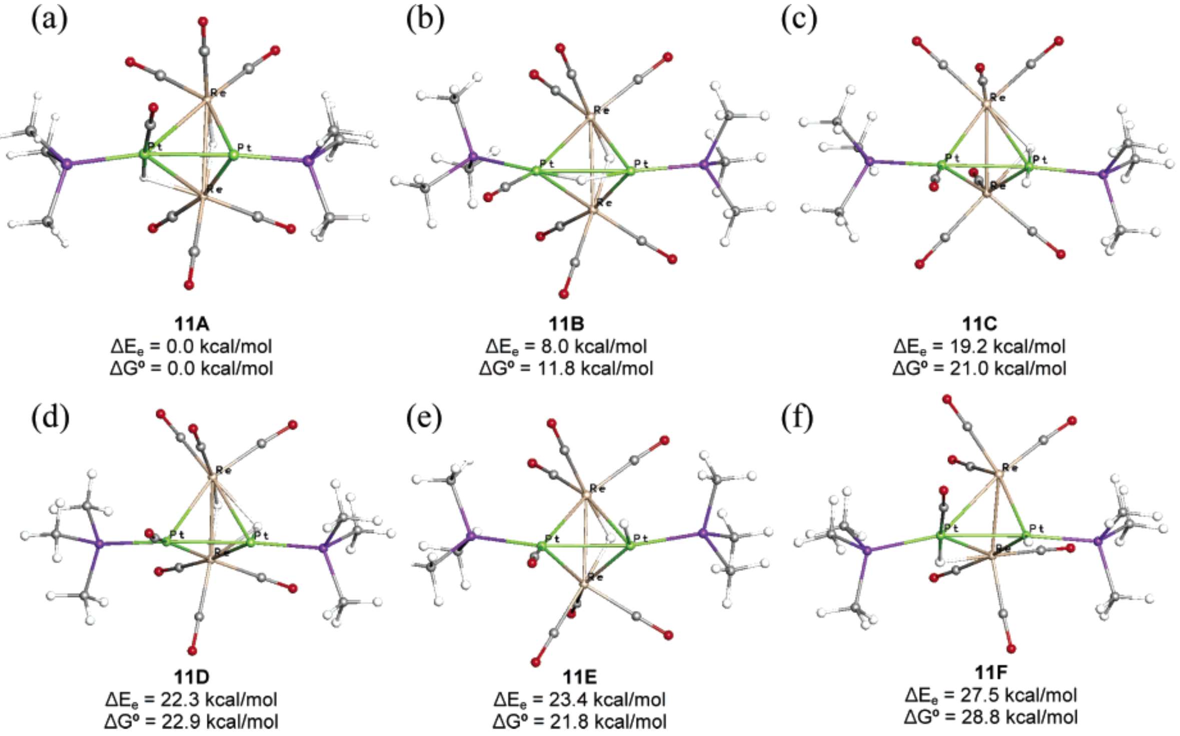

11A
ΔE_e = 0.0 kcal/mol
ΔG^o = 0.0 kcal/mol

11B
ΔE_e = 8.0 kcal/mol
ΔG^o = 11.8 kcal/mol

11C
ΔE_e = 19.2 kcal/mol
ΔG^o = 21.0 kcal/mol

11D
ΔE_e = 22.3 kcal/mol
ΔG^o = 22.9 kcal/mol

11E
ΔE_e = 23.4 kcal/mol
ΔG^o = 21.8 kcal/mol

11F
ΔE_e = 27.5 kcal/mol
ΔG^o = 28.8 kcal/mol

Figure 5. QM model optimized structures and relative energies for **11**. Relative energies compared to the lowest energy structure, **11A** (0.0 kcal/mol). Platinum (green), rhenium (beige), phosphorus (purple), oxygen (red), carbon (gray), hydrogen (white).

coordination rearrangements of CO ligands have been known for many years and are well-known to be facile.[29] The hydrido ligand that bridges the Pt−Re bond will also have to shift to a symmetrically equivalent Pt−Re bond involving the other Pt atom. The facile shifting of the hydrido ligands in **11** was established by the ^{1}H NMR spectra, Figure 4.

It is known that cluster complexes can have less than the expected number of valence electrons in the presence of platinum atoms because of the tendency of platinum to adopt 16 electron configurations. Tetrahedral Pt_2M_2 compounds often have 58 valence electrons.[30] However, a decrease to 54 electrons, as found in **11**, is very unusual and suggests a high degree of electronic unsaturation. The unsaturation may be tied to the presence of the bulky PBu^t_3 ligands which inhibits the addition of other ligands, such as CO, that would ordinarily provide additional electrons to the metal atoms.

A number of geometry optimized structures were calculated for **11** by using the B3PW91 DFT method by placing the hydrido ligands in various bridging positions along the metal−metal bonds. These results are shown in Figure 5. The most stable structure is **11A** which has two bridging hydrido ligands: one along the Re−Re bond and one along the Re(1)−Pt(1) bond as labeled in Figure 3. It is also worth noting that the structure **11A** is also the only optimized structure that accurately reproduces the arrangement of the nonhydrogen ligands for **11** as established by the crystal structure analysis. It is therefore assumed that this structure has the correct arrangement for the hydrido ligands.

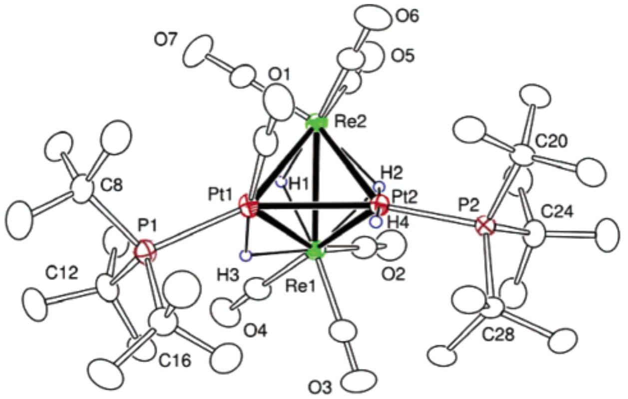

Figure 6. An ORTEP diagram of the molecular structure of **12** showing 40% probability thermal ellipsoids. Selected interatomic distances (Å) are as follows: Pt(1)−Pt(2) = 2.7025(2); Pt(1)−Re(1) = 2.9732(2); Pt(1)−Re(2) = 2.8805(2); Pt(2)−Re(1) = 2.9182(2); Pt(2)−Re(2) = 2.7866(2); Re(1)−Re(2) = 2.8303(3); Pt(1)−H(3) = 1.50(7); Pt(2)−H(2) = 1.78(6), Pt(2)−H(4) = 1.51(5), Re(1)−H(1) = 1.74(4), Re(1)−H(2) = 2.03(6), Re(1)−H(3) = 2.02(7), Re(2)−H(1) = 1.89(4); Re(2)−H(2) = 1.95(6); Pt(1)−P(1) = 2.3909(10); Pt(2)−P(2) = 2.2729(9).

Because of the unusually facile addition of hydrogen to the unsaturated five metal cluster complex **6**,[7] we were prompted to investigate the reactivity of **11** with hydrogen. Interestingly, it was found that **11** reacts with hydrogen at room temperature to yield the tetrahydrido complex $Pt_2Re_2(CO)_7(PBu^t_3)_2(\mu\text{-}H)_4$, **12**, in 71% isolated yield after a 12 h reaction period. Compound **12** was characterized by IR, ^{1}H and ^{31}P NMR spectroscopy, mass spectrometry, and single-crystal X-ray diffraction analyses. An ORTEP diagram of the molecular structure of **12** is shown in Figure 6. The structure of the cluster **12** is very similar to that of **11**. The four metal atoms are arranged in the form of a tetrahedron. The seven CO ligands are distributed among the metal atoms similarly to those in **11**, and as in **11** each platinum atom contains one PBu^t_3 ligand.

---

(28) Churchill, M. R.; Lashewycz, R. A.; Shapley, J. R.; Richter, S. I. *Inorg. Chem.* **1980**, *19*, 1277−1285.

(29) Adams, R. D.; Cotton, F. A. *Dynamical Nuclear Magnetic Resonance Spectroscopy*; Academic Press: 1975.

The presence of the four hydrido ligands was confirmed by its mass spectrum, $m/e = 1367$, and further supported by the ^{1}H NMR spectrum; see below. In addition, the structural analysis of **12** was of much better quality than that of **11**, and in this analysis each of the four hydrido ligands was located and refined crystallographically. Two of the hydrido ligands occupy positions similar to those proposed for **11**; that is, one H(1) bridges the Re−Re bond and one H(3) bridges the Pt(1)−Re(1) bond. The other two hydrido ligands are associated with Pt(2). H(2) is a triply bridging ligand that is bonded to Pt(2), Re(1), and Re(2); Pt(2)−H(2) = 1.78(6) Å, Re(1)−H(2) = 2.03(6) Å, Re(2)−H(2) = 1.95(6) Å. H(1) is terminally coordinated to Pt(2), Pt(2)−H(4) = 1.51(5) Å. As expected the Pt−H bond distance of the terminally coordinated hydrido ligand is significantly shorter than that for bridging hydrido ligands.[25] The hydride bridged metal−metal bonds in **12** are all significantly longer than those in **11**, Pt(2)−Re(1) = 2.9182(2) Å; Pt(2)−Re(2) = 2.7866(2) Å.[25] The Pt(1)−Re(1) bond distance, 2.9732(2) Å, is longer than that in **11**, but the Re−Re distance is slightly shorter, Re(1)−Re(2) = 2.8303(3) Å. The Pt(1)−Re(2) bond in **12** is slightly longer than that in **11**, 2.8805(2) Å.

The ^{1}H NMR spectrum of **12** exhibits three high field resonances, −2.13, −2.34, and −6.10 ppm in a 1/1/2 ratio, consistent with the presence of four hydrido ligands, but this is not completely consistent with the solid-state structure which shows four inequivalent hydrido ligands. Low temperature measurements of the ^{1}H NMR spectra of **12** showed a substantial broadening of the hydride resonance at −6.10 ppm which suggests that this may be a dynamically averaged resonance, but this could not be resolved into its components at the lowest temperatures that we could achieve on our spectrometer (−85 °C).

To test for the presence of a kinetic isotope effect in the addition of hydrogen to **11**, we compared the rates of addition of H_2 and D_2 to **11** as a function of time. A significant isotope effect, D/H isotope effect of 1.5(1), was determined by following the rates of formation of **12** and **12-d$_2$** from **11** by IR spectroscopy. This suggests that the activation of H_2 may occur at or before the slow step of the reaction.

Mechanism of Hydrogen Addition to 11. Molecular orbital calculations were performed to try to shed some light on the mechanism of the addition of H_2 to **11**. Figure 7 shows a contour diagram of the Fenske−Hall LUMO of **11**. It shows that a major component of the orbital is found on the platinum atom Pt(2), shown in Figure 3, which strongly suggests that this atom is a likely site for the H_2 addition. It is also the atom which is most strongly associated with the two added hydrido ligands in the product **12**. Accordingly, optimized structures to test the mode of addition of H_2 to this atom were investigated by using the B3PW91 DFT method and a computational model in which PMe_3 ligands were used in place of P(t-Bu)$_3$ ligands. Figure 8 shows a pathway of geometry optimized structures for the addition of H_2 to the platinum atom Pt(2) in **11** to form **12**. The addition begins by coordination of dihydrogen to **11A** to form an **η^1-H$_2$** complex, **11-η^1-H$_2$** (Figure 8b). Next, the dihydrogen ligand changes coordination modes via **TS-η^1-H$_2$ → η^2-H$_2$** (Figure 8c) to form the **η^2-H$_2$** complex, **11-η^2-H$_2$** (Figure 8d). From **11-η^2-H$_2$**, addition of dihydrogen proceeds through the transition state, **TS-η^2-H$_2$ → 12B** (Figure 8e), to yield complex **12B** (Figure 8f), in which the H−H distance has increased to 1.571 Å. The structure and energy of **TS-η^2-H$_2$ → 12B** were estimated from the highest energy point on a relaxed potential energy scan starting from **12B**, from which the H−H distance was reduced in increments of 0.05 Å. This relaxed potential energy scan revealed the highest electronic energy was obtained at a H−H distance of 1.421 Å, and thus, this point was used as **TS-η^2-H$_2$ → 12B**. However, it should be noted that the electronic energy of **TS-η^2-H$_2$ → 12B** is only 0.05 kcal/mol higher than the electronic energy of **12B**; thus, **12B** is a very shallow minima on the potential energy surface. The final product, **12A** (Figure 8h), is generated from **12B** via the transition state **TS-12B → 12A** (Figure 8g). Nocera has recently shown that hydrogen adds selectively to a single metal site in some mixed valence diiridium complexes.[31]

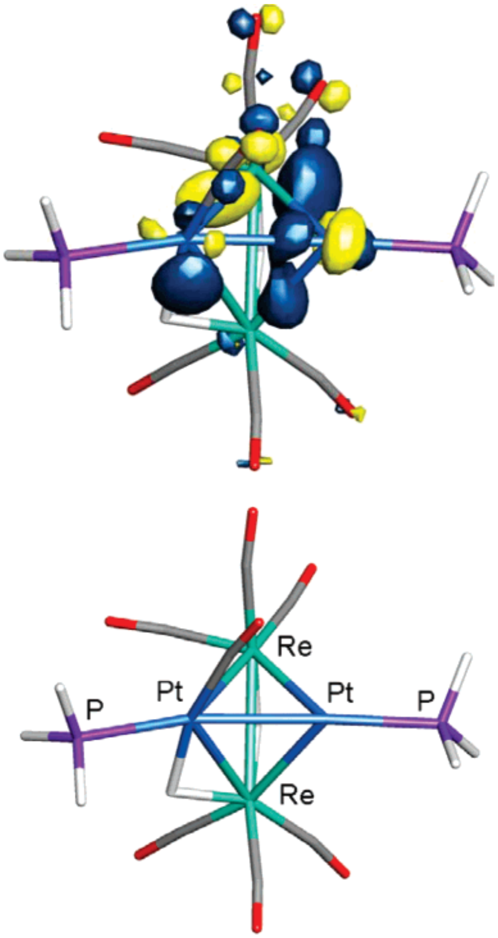

Figure 7. A contour plot of the Fenske−Hall lowest unoccupied molecular orbital (LUMO) of **11** (top) and labeling diagram (bottom).

Interestingly, compound **12** readily eliminates 1 equiv of hydrogen when heated to 97 °C to regenerate **11** in 90% isolated yield. Similarly, the elimination of H_2 from **12** to yield **11** can be induced at room temperature by the application of UV−vis irradiation to solutions of **12**. The hydrogen that was eliminated was verified as H_2 by its characteristic ^{1}H NMR resonance at $\delta = 4.51$ observed in solutions of **12** that were heated to 100 °C

---

(30) (a) Farrugia, L. J. *Adv. Organomet. Chem.* **1990**, *31*, 301−391. (b) Adams, R. D.; Captain, B.; Fu, W.; Hall, M. B.; Smith, M. D.; Webster, C. E. *Inorg. Chem.* **2004**, *43*, 3921−3929.

(31) (a) Gray, T. G.; Veige, A. S.; Nocera, D. G. *J. Am. Chem. Soc.* **2004**, *126*, 9760−9768. (b) Veige, A. S.; Gray, T. G.; Nocera, D. G. *Inorg. Chem.* **2005**, *44*, 17−26.

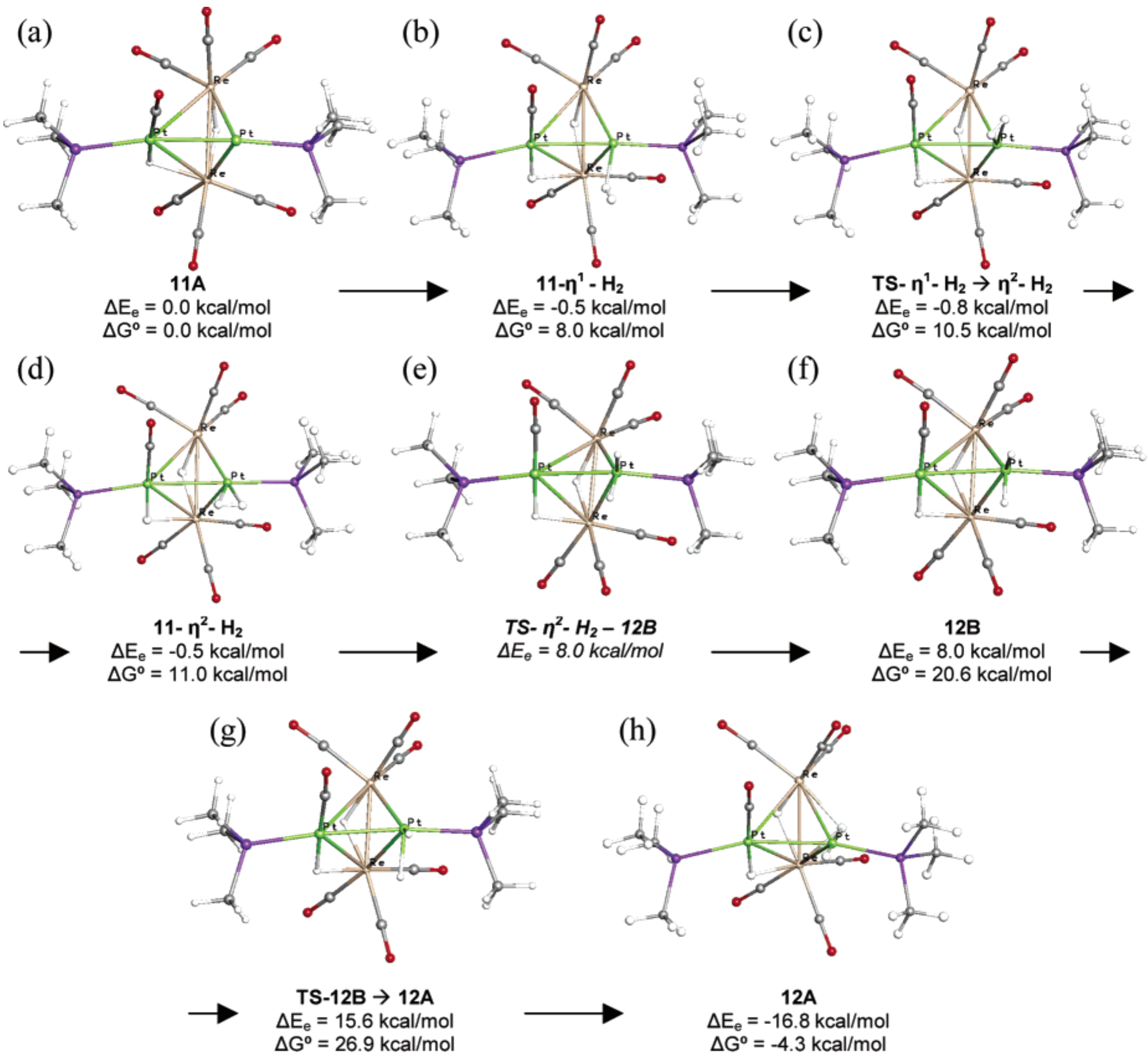

Figure 8. QM optimized dihydrogen complexes, transition states for H_2 activation, and resulting local minima for the **11** + **H_2** at Pt: (a) **11A**, (b) **11-η^1-H_2**, (c) **TS-η^1-H_2 → η^2-H_2**, (d) **11-η^2-H_2**, (e) **TS-η^2-H_2 → 12B**, (f) **12B**, (g) **TS-12B → 12A**, and (h) **12**. Relative energies of the **11-H_2**−Pt series (a−h) are compared to the lowest energy **11** complex + separated H_2 = 0.0 kcal/mol. The structure and relative energy of (e) **TS-η^2-H_2 → 12B** were estimated from the highest energy structure of a relaxed potential energy scan starting from **12B**, in which the H−H distance was decreased in increments of 0.05 Å. All other structures were fully optimized. Platinum (green), rhenium (beige), phosphorus (purple), oxygen (red), carbon (gray), hydrogen (white).

or subjected to UV−vis irradiation at room temperature. The mechanism for the thermal elimination of H_2 from **12** is assumed to be the microscopic reverse of the addition process shown in Figure 8.

Because **12** is also electronically unsaturated, it was decided to investigate its reaction with CO. Compound **12** was found to react with CO in heptane solvent at room temperature to yield the new compound $Pt_2Re_2(CO)_8(PBu^t_3)_2(\mu\text{-}H)_4$, **13**, in 73% yield within 2 h. Compound **13** was characterized by IR, ^{1}H and ^{31}P NMR spectroscopy, mass spectrometry, and single-crystal X-ray diffraction analyses. An ORTEP diagram of the molecular structure of **13** is shown in Figure 9. The molecule contains a crystallographically imposed center of symmetry in the solid state. The structure of **13** has a planar cluster of four metal atoms, two of platinum and two of rhenium, in the shape of a rhombus. There is a bond between the two diagonally positioned platinum atoms, Pt(1)−Pt(1*) = 2.7140(2) Å. Each rhenium atom contains four linear terminal carbonyl ligands, and each platinum atom contains one PBu^t_3 ligand. Compound **13** contains four hydrido ligands that bridge each of the four Pt−Re bonds around the periphery of the cluster, Pt(1)−H(1) = 1.59(4) Å,

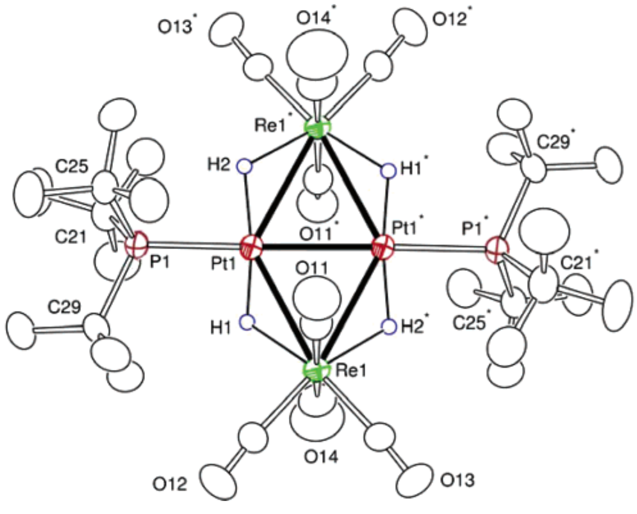

Figure 9. An ORTEP diagram of the molecular structure of **13** showing 40% probability thermal ellipsoids. Selected interatomic distances (Å) and angles (deg) are as follows: Pt(1)−Pt(1*) = 2.7140(2), Pt(1)−Re(1) = 2.8801(2), Pt(1)−Re(1*) = 2.8879(2), Pt(1)−H(1) = 1.59(4), Pt(1)−H(2) = 1.69(4), Re(1)−H(1) = 1.88(4).

Scheme 2

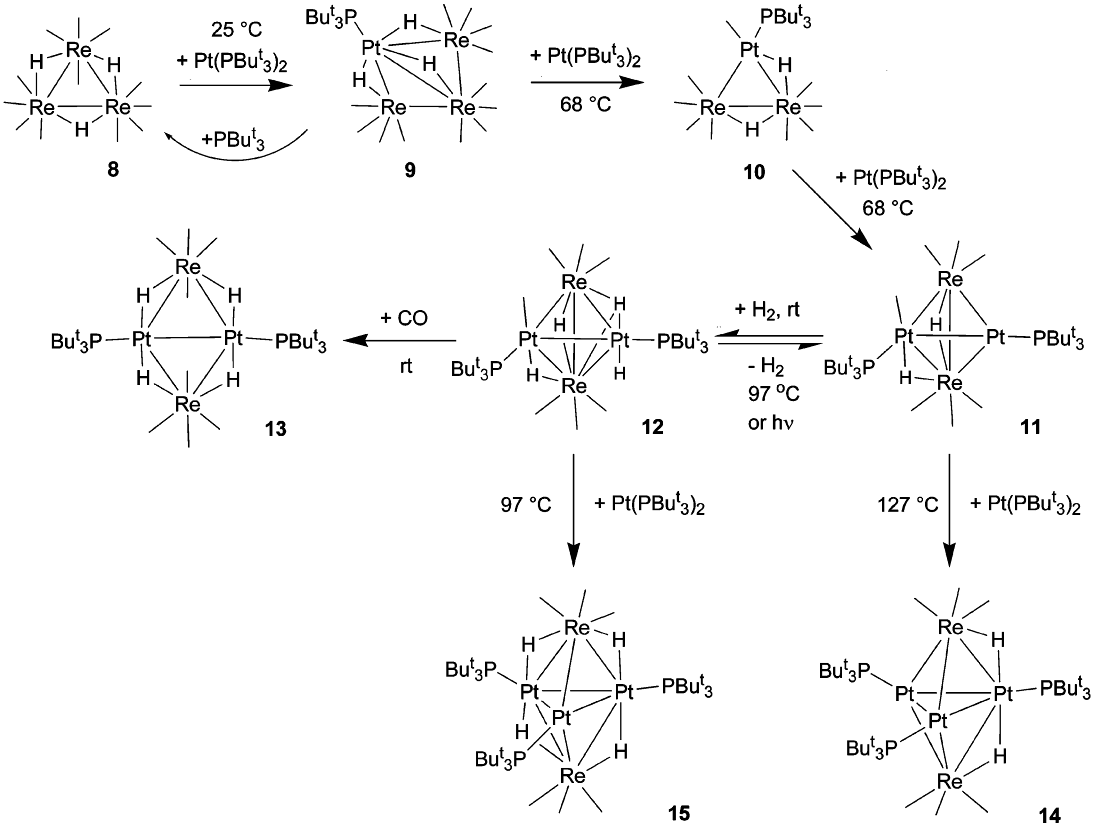

Pt(1)−H(2) = 1.69(4) Å, Re(1)−H(1) = 1.88(4) Å. These Pt−Re bonds are similar in length to the hydride bridged Pt−Re bonds in **11**and **12**, Pt(1)−Re(1) = 2.8801(2) Å and Pt(1)−Re(1*) = 2.8879(2) Å. The hydrido ligands are all equivalent and appear as a single resonance at −6.27 ppm with appropriate ^{195}Pt and ^{31}P couplings, ^1J(Pt,H) = 683 Hz, ^2J(P,H) = 7 Hz in the ^{1}H NMR spectrum. Compound **13** contains a total of 58 cluster valence electrons which is four less than that required for such a structure in which all the metal atoms have 18 electron configurations. This can be explained for **13** if the two platinum atoms have 16 electron configurations.

When **11** and **12** were treated with additional quantities of Pt(PBu$^t_3$)$_2$, they were enlarged to yield the triplatinumdirhenium complexes Pt$_3$Re$_2$(CO)$_6$(PBu$^t_3$)$_3$(μ-H)$_2$, **14**, and Pt$_3$Re$_2$(CO)$_6$(PBu$^t_3$)$_3$(μ-H)$_4$, **15**, respectively. These unsaturated cluster complexes, which also add hydrogen at room temperature, have recently been described by us in another report and will not be further described herein.[7a]

Summary and Conclusions

A summary of the reactions described in this report are shown in Scheme 2. It has been shown for the first time that the Pt(PBu$^t_3$) group can be inserted into the hydride-bridged Re−Re bond of **8** to yield the adduct **9** as the first step in a metal substitution process that leads to the trinuclear PtRe$_2$ complex **10**. Compound **10** reacts with Pt(PBu$^t_3$)$_2$ to yield the highly unsaturated four metal Pt$_2$Re$_2$ complex **11** that adds hydrogen *reversibly* under mild conditions to yield the tetrahydrido Pt$_2$Re$_2$ complex **12**. Molecular orbital calculations suggest that the H$_2$ addition occurs at the platinum atom with the lower coordination. Compound **12** which is also unsaturated was found to add CO to yield the open cluster complex **13**. Compound **11** and **12** add yet another platinum atom to yield the five metal cluster complexes **14** and **15**.[7]

Recent studies have shown that heteronuclear metallic nanoparticles prepared from mixed metal carbonyl cluster complexes containing platinum exhibit superior properties as hydrogenation catalysts.[32] Our studies suggest that ligand deficient platinum atoms are the preferred sites for hydrogen activation in unsaturated mixed metal cluster complexes. They may also be prime sites for hydrogen activation on platinum containing ligand-free heteronuclear nanoparticles on supports.

Acknowledgment. This research was supported by the Office of Basic Energy Sciences of the U.S. Department of Energy under Grant No. DE-FG02-00ER14980 and the USC Nanocenter. We thank Dr. Perry J. Pellechia for assistance with the variable temperature NMR measurements. Dedicated to the memory of F. Albert Cotton, a true friend and leader.

Supporting Information Available: CIF files for each of the structural analyses are available. Also complete citation for ref 13. This material is available free of charge via the Internet at http://pubs.acs.org.

JA070773O

---

(32) (a) Hungria, A. B.; Raja, R.; Adams, R. D.; Captain, B.; Thomas, J. M.; Midgley, P. A.; Golvenko, V.; Johnson, B. F. G. *Angew. Chem., Int. Ed.* **2006**, *45*, 4782−4785. (b) Thomas, J. M.; Johnson, B. F. G.; Raja, R.; Sankar, G.; Midgley, P. A. *Acc. Chem. Res.* **2003**, *36*, 20−30. (c) Hermans, S.; Raja, R.; Thomas, J. M.; Johnson, B. F. G.; Sankar, G.; Gleeson, D. *Angew. Chem., Int. Ed.* **2001**, *40*, 1211−1215.